Accelerated Publication

THE JOURNAL OF BIOLOGICAL CHEMISTRY
Vol. 277, No. 16, Issue of April 19, pp. 13363–13366, 2002

Solution Structure of Human $GABA_A$ Receptor-associated Protein GABARAP

IMPLICATIONS FOR BIOLOGICAL FUNCTION AND ITS REGULATION*

Received for publication, January 25, 2002,
and in revised form, February 27, 2002
Published, JBC Papers in Press, March 1, 2002,
DOI 10.1074/jbc.C200050200

Thomas Stangler‡§, Lorenz M. Mayr¶, and Dieter Willbold§‖**

From the ‡Institut für Molekulare Biotechnologie, Beutenbergstr. 11, 07745 Jena, Germany, the §Institut für Physikalische Biologie, Heinrich-Heine-Universität, 40225 Düsseldorf, Germany, ¶Novartis Pharma AG, CH-4002 Basel, Switzerland, and ‖Forschungszentrum Jülich, IBI-2, 52425 Jülich, Germany

Control of neurotransmitter receptor expression and delivery to the postsynaptic membrane is of critical importance for neural signal transduction at synapses. The γ-aminobutyric acid, type A ($GABA_A$) receptor-associated protein GABARAP was reported to have an important role for movement and sorting of $GABA_A$ receptor molecules to the postsynaptic membrane. GABARAP not only binds to $GABA_A$ receptor γ2-subunit but also to tubulin, gephyrin, and ULK1. We present for the first time the high resolution structure of human GABARAP determined by nuclear magnetic resonance in aqueous solution. One part of the molecule, despite being well ordered and rigid on a MHz time scale, exists in at least two different conformations that interchange with each other on a time scale slower than 25 Hz. An important feature of the solution structure is the observation that amino- and carboxyl-terminal ends of the protein directly interact with each other, which is not seen in recently reported crystal structures. The possible biological relevance of these observations for the regulation of GABARAP interactions and functions is discussed.

Rapid signaling at synapses between neurons are mediated by small molecules called neurotransmitters. Among neurotransmitters, the most prominent are acetylcholine and glutamate for excitatory synapses and glycine and γ-amino butyric acid (GABA)[1] for inhibitory synapses, respectively. Receptors for these neurotransmitters are important targets for drugs used to treat mental disorders or to modulate sleep and mood. The principal GABA-gated ion channel is the GABA type A ($GABA_A$) receptor. Drugs that bind to $GABA_A$ receptors and modulate their activity, such as the benzodiazepines, offer both medical and economic potential.

Control of neurotransmitter receptor expression at the postsynaptic membrane is of critical importance for functional neurotransmission. Sorting, targeting, clustering, and degradation of neurotransmitter receptors as dynamic processes play a key role in the construction and functional maintenance of synapses.

Recently a novel protein was identified as a binding partner for the γ2-subunit of $GABA_A$ receptor, termed GABARAP ($GABA_A$ receptor-associated protein) (1). GABARAP is also reported to bind tubulin (1), gephyrin (2), and ULK1 (3). It is closely related to light chain-3 (LC-3) of microtubule-associated proteins 1A and 1B (MAP-1A and -1B) and to the "late acting intra-Golgi transport factor," termed GATE-16, of which crystal structures are known (4). In contrast to GABARAP, however, GATE-16 does not interact with gephyrin and $GABA_A$ receptor γ2-subunit (2). GABARAP is postulated to have an important role for early steps in movement and sorting of $GABA_A$ receptors (5) and for $GABA_A$ receptor clustering at the postsynaptic membrane. Binding affinity of GABA to $GABA_A$ receptors as well as kinetics of inactivation and desensitization of the receptors are dependent on the clustering state of the GABA receptor, which was reported to be strongly modulated by GABARAP (6). Modulation of GABARAP binding to its interaction partners provides a new avenue for pharmacological intervention of receptor activity and neurotransmitter action at the synapse. We and others therefore started a detailed structural investigation of GABARAP. The first available crystal structure of GABARAP (7) turned out to be very similar to the crystal structures of GATE-16 (4), which is not very surprising since sequence identity between both proteins is 57%. GATE-16 and the GABARAP crystal structures resemble ubiquitin folds with two additional amino-terminal helices. A difference in GATE-16 in the putatively flexible carboxyl-terminal residues and smaller differences in helix 2 and loop regions were found. An additional two different crystal structures of GABARAP are reported but not deposited in the Protein Data Bank (8) rendering them impossible to be studied in detail and compared with other structures. Coyle *et al.* (8) obtained the structures from two different crystal forms. One structure is reported to resemble closely that of GATE-16. The other crystal form was obtained under high salt conditions in which helix 1 is flipped by ~180°, pointing away from the rest of the molecule and contacting the neighboring molecule in the crystal in a head to tail fashion. Whether this polymerized state of GABARAP might be of physiological relevance is not clear.

EXPERIMENTAL PROCEDURES

Protein Expression and Purification—GABARAP was expressed and purified as a glutathione *S*-transferase fusion protein. Thrombin (Merck) cleavage was performed yielding full-length GABARAP with additional glycine and serine residues at its amino terminus. Details of

* The costs of publication of this article were defrayed in part by the payment of page charges. This article must therefore be hereby marked "*advertisement*" in accordance with 18 U.S.C. Section 1734 solely to indicate this fact.

The atomic coordinates and structure factors (code 1KOT) have been deposited in the Protein Data Bank, Research Collaboratory for Structural Bioinformatics, Rutgers University, New Brunswick, NJ (http://www.rcsb.org/).

** To whom correspondence should be addressed. Tel.: 49-2461-612100; Fax: 49-2461-612023; E-mail: dieter.willbold@uni-duesseldorf.de.

[1] The abbreviations used are: GABA, γ-aminobutyric acid; $GABA_A$, GABA type A; GABARAP, $GABA_A$ receptor-associated protein; LC-3, light chain-3; MAP, microtubule-associated protein; NOE, nuclear Overhauser effect; NOESY, NOE spectroscopy; HSQC, heteronuclear single quantum correlation; r.m.s.d., root mean square deviation; E1, ubiquitin-activating enzyme.

cloning, protein expression, and purification of GABARAP have been described elsewhere (9).

NMR Spectroscopy—NMR samples contained 0.8 mM protein in 25 mM sodium phosphate, 100 mM NaCl, 100 mM KCl, pH 6.9, in 95% H_2O, 5% D_2O with 100 μM phenylmethylsulfonyl fluoride, 0.02% (by weight) sodium azide, and 50 μM EDTA. NMR spectra were recorded at 298 K on a Varian Unity INOVA spectrometer equipped with a triple-axis pulse-field gradient $^1H/^{15}N/^{13}C$ probe at proton frequencies of 600 and 750 MHz. The resonance assignment of GABARAP was described previously (9). Structural constraints were derived from ^{15}N-edited NOESY-HSQC (100-ms mixing time) (10), aliphatic ^{13}C-edited NOESY-HSQC (80-ms) experiments (11) in the described buffer, and aliphatic ^{13}C-edited NOESY-HSQC (120-ms) and aromatic ^{13}C-edited NOESY-HSQC (120-ms) experiments with protein in the buffer after replacement of H_2O by D_2O. Uniformly ^{13}C-^{15}N-labeled protein was used for these experiments. ^{15}N-Labeled protein was used for the ^1H-^{15}N heteronuclear NOE experiments (12).

Data Evaluation and Structure Calculation—Based on the almost complete assignment of ^1H, ^{13}C, and ^{15}N resonances of GABARAP, a total of 4577 NOE distance constraints (including 1375 long range NOEs) could be derived from three-dimensional NOESY spectra in an iterative procedure (Table I). NOE analysis and assignment were performed using NMRView (13) and ARIA (14). Interproton distances were used directly to calibrate experimental peaks and to extract distance constraints. Lower and upper bounds for distance constraints were derived from the target distances empirically by estimation of the error as 12.5% of the target distance squared. Distances involving ambiguous constraints, methyl groups, aromatic ring protons, and the nonstereospecifically assigned methylene protons were treated as sum of separate contributions to the target function, known as "sum averaging" (15).

Final structures were calculated using the simulated annealing protocol with the program CNS version 1.0 (16) using standard parameters with the following modifications. For conformational space sampling 20 ps with a time step of 10 fs were simulated using torsion angle dynamics at a temperature of 50,000 K followed by 30 ps of slow cooling to 0 K with a time step of 15 fs. In an additional Cartesian slow cooling stage, the temperature was decreased in 20 ps from 2000 to 0 K with a time step of 5 fs. After simulated annealing the structures were subjected to 2000 steps of energy minimization.

A total of 15 structures that did not show any distance constraint violation of more than 0.0175 nm was used for further analysis. Geometry of the structures, structural parameters, and secondary structure elements were analyzed and visualized using the programs MOLMOL (17), PROCHECK (18), and WHATIF (19). The coordinates have been deposited in the Protein Data Bank with accession code 1KOT.

RESULTS AND DISCUSSION

Solution Structure and Comparison with Crystal Structures of GABARAP and GATE-16—Earlier we reported almost complete assignments for backbone and side chain ^1H, ^{13}C, and ^{15}N resonances of human GABARAP (9). Simultaneously backbone resonance assignments were reported by others (20). Reinspection of the spectra allowed us to increase especially the extent of backbone ^1H and ^{15}N amide resonance assignments to 98%. Only amide resonances of Val^6 and Asp^{102} eluded their assignment.

A total of 4577 NOE distance constraints, including 1375 long range NOEs (Table I), derived from three-dimensional ^{15}N- or ^{13}C-edited NOESY spectra recorded from uniformly ^{15}N and ^{13}C isotope-labeled recombinantly expressed GABARAP protein was taken as input for simulated annealing and refinement calculations. No other constraints were used. Together 15 structures were obtained that did not show any NOE distance violation greater than 0.0175 nm. The root mean square deviation of these 15 structures relative to their average structure was 0.049 and 0.105 nm for backbone and all heavy atoms, respectively. That means the resulting structure is rather well defined as seen in the overlay of all 15 protein backbones (Fig. 1*A*).

The structure of GABARAP exhibits a compact fold consisting of a four-stranded β-sheet with two α-helices on either side (Fig. 1*B*). Similar to the ubiquitin fold, the outer strands of the

TABLE I
Constraints and structural statistics for the resulting 15 NMR structures of GABARAP

Number of experimental restraints	
Total number of assigned NOEs	4577
Intraresidue ($\|i - j\| = 0$)	1448
Interresidue sequential ($\|i - j\| = 1$)	885
Interresidue medium range ($1 < \|i - j\| \leq 5$)	869
Long range ($\|i - j\| > 5$)	1375
CNS energies (kcal/mol)	
Total	259.19 ± 5.91
Bond	12.08 ± 0.53
Angle	95.04 ± 2.76
Impropers	12.85 ± 0.79
van der Waals	99.55 ± 3.58
NOE	39.68 ± 2.17
r.m.s.d. to the mean structure (nm)	
Backbone heavy atoms	0.049 ± 0.017
All heavy atoms	0.105 ± 0.014
r.m.s.d. to experimental constraints and idealized geometry	
NOE (nm)	0.00097 ± 0.00002
Bond (nm)	0.00024 ± 0.00001
Angle (°)	0.4126 ± 0.0060
Impropers (°)	0.2791 ± 0.0086
Φ, Ψ angles consistent with Ramachandran plot (%)	
Most favored regions	72.6
Allowed regions	96.8
Generously allowed regions	98.4

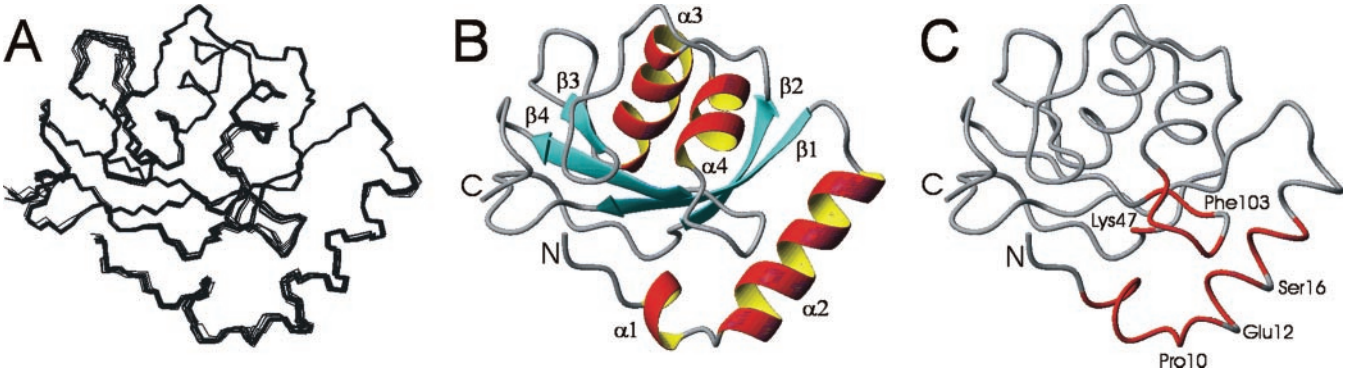

FIG. 1. **Solution structure of human GABARAP after simulated annealing and refinement calculations.** *A*, shown is the superposition of the backbones of all 15 obtained structures. *B*, ribbon presentation of the averaged GABARAP structure. Secondary structure elements are labeled according to their sequential arrangement. Amino- (*N*) and carboxyl (*C*)-terminal ends are indicated. *C*, backbone worm presentation of GABARAP. Residues that contain amide groups with split or broadened resonance peaks are colored in *red*. Residues Val^6 and Asp^{102} are also colored in *red* because their amide resonances were undetectable. This indicates that the respective residues are involved in conformational exchange on a slow to intermediate time scale. Prominent residues are labeled with amino acid type and sequence position. All figures were prepared using MOLMOL (17).

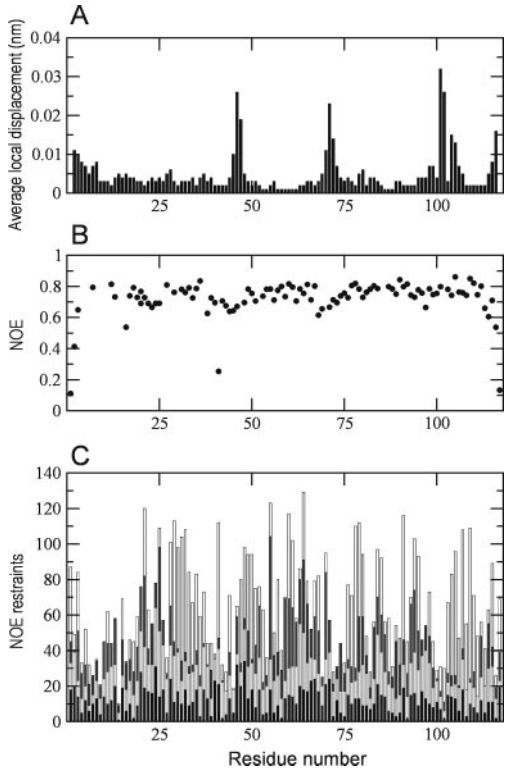

FIG. 2. **Precision of local conformation, dynamic behavior, and number of distance constraints per residue.** *A*, average local displacement values among the 15 obtained solution structures. For each three-residue window the average displacement of the backbone atoms was calculated and plotted against the residue number that corresponds to the central residue of the window. *B*, heteronuclear ^{1}H-^{15}N NOE values of amide resonances. *C*, number of intraresidual (*black*), sequential (*light gray*), medium (*dark gray*), and long range (*white*) NOE distance constraints per residue.

β-sheet are aligned antiparallel to the inner strands, which are parallel to each other, and helices α3 and α4 are located on one side of the sheet. In addition to the ubiquitin fold, GABARAP contains two additional helices, α1 and α2, that are located on the opposite side of the β-sheet relative to α3 and α4.

Average local displacement values relative to the mean structure are a measure for the precision of the derived family of structures. Large values indicate either local flexibility of the protein or lack of experimental data for this region. Average local displacement values of the GABARAP solution structure indicate the regions Asp^{45}–Lys^{47}, Leu^{70}–Glu^{73}, and Glu^{101}–Leu^{105} of the protein to be less defined (Fig. 2*A*). The first two regions also have slightly decreased heteronuclear NOE values (Fig. 2*B*) indicating increased dynamic behavior. ^{1}H-^{15}N heteronuclear amide NOE values are a measure for the dynamics of the local environment within the time scale of the absolute NMR frequencies (60–750 MHz in the present study).

Overall the solution structure is very similar to that of the GABARAP crystal structure (7). Notable differences between the solution structure and all deposited crystal structures of GABARAP and GATE-16 map to residues 2–14, 37–46, 66–75, and 113–117. The first region largely overlaps with residues that appear in the NMR spectra as broadened and split resonances. Regions 37–46 and 66–75 coincide with those shown to have slightly increased mobility as inferred from heteronuclear NOE data (Fig. 2*B*).

The root mean square deviation (r.m.s.d.) value for the backbone coordinates of residues 1–112 is 0.134 nm between GABARAP solution and crystal structure (7) as well as 0.139 and 0.151 nm for GABARAP solution structure and GATE-16

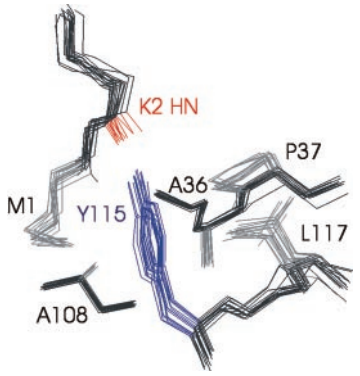

FIG. 3. **Focused view of the GABARAP structure.** Shown is the superposition of the backbone atom connections of residues Met^{1}, Lys^{2}, Ala^{36}, Pro^{37}, Ala^{108}, and Tyr^{115}–Leu^{117} (all in *black*) for all obtained structures. The side chains of Met^{1}, Ala^{36}, Pro^{37}, Ala^{108}, and Leu^{117} (*gray*) form a hydrophobic pocket for the side chain of Tyr^{115} (*blue*). The hydroxyl oxygen of the Tyr^{115} phenolic ring is hydrogen-bonded to the backbone amide nitrogen of Lys^{2} (*red*).

crystal structures (4). The coordinates for the very carboxyl-terminal residues, however, differ remarkably.

Some Regions of GABARAP Are Involved in Conformational Exchange—Backbone amide resonances of a number of residues showed up in the NMR spectra as broadened and split lines, indicating conformational exchange on an intermediate and slow time scale. Due to the lack of concentration dependence, the observed phenomenon could not be assigned to a monomer-dimer equilibrium. The respective residues map to completely different sequence regions (Val^{4}–Lys^{20} without Glu^{12} and Ser^{16}, His^{99}–Leu^{105} without Phe^{103}, and Lys^{47}) that are all close to each other in space (Fig. 1*C*). The first region encompasses helix α1 and a large portion of helix α2, and the second region belongs to the loop between helix α4 and strand β4. The carboxyl-terminal Leu^{105} of the second region exhibits a split backbone amide resonance, but the corresponding proton is involved in stable β-sheet-like secondary structure hydrogen bonding with the Pro^{30} backbone carbonyl oxygen as suggested by inspection of the structure and the stability of the Leu^{105} amide proton in hydrogen exchange experiments (data not shown). Lys^{47} is located next to the amino terminus of strand β2, and its side chain protrudes to the amino terminus of helix α1, thus obviously opposing the dipole of helix α1. Phe^{103}, Glu^{12}, and Ser^{16} appear not to be affected by line broadening or splitting. Also the amino-terminal residues Met^{1}, Lys^{2}, and Phe^{3} are not visibly affected by conformational exchange phenomena. To estimate the time scale for a potential exchange between the different conformations corresponding to the different observed sets of resonances, the frequency distance for several pairs of split amide resonances were measured. Some of them (Arg^{15} and Lys^{20}) yielded values of 25 and 27 Hz, respectively. That leads to the conclusion that, under the conditions used in the present study, any exchange between the conformers is slower than 25 Hz.

Interestingly all residues involved in this conformational exchange are spatially close to Pro^{10}. This residue is discussed as the hinge for the interchange between two different conformations yielded for GABARAP under different crystallization conditions (8). Comparing both conformations relative to each other, helix α1 is flipped by ~180° at residue Pro^{10}. The potential of conformational changes around Pro^{10} is principally in accordance with the dynamics observations obtained for the GABARAP solution structure. However, the proposed head to tail polymerization could not be observed under the conditions used in the present study.

The Carboxyl-terminal Part of GABARAP Is Well Defined and in Direct Contact with the Amino-terminal Residues—

GABARAP and GATE-16 crystal structures indicate that the carboxyl-terminal part of the respective molecule is not an integral part of the protein scaffold. In the publicly accessible crystal structures of GABARAP and the two GATE-16 conformers the carboxyl termini differ significantly among themselves and compared with the solution structure. This may be due to different favorable crystal contacts of the carboxyl-terminal end observed in the crystal structures (4, 7). Inspection of the solution structure of GABARAP reveals that the hydroxyl oxygen of the Tyr^{115} phenolic ring is hydrogen-bonded to the backbone amide nitrogen of Lys^{2} (Fig. 3). Furthermore Tyr^{115} is involved in a network of hydrophobic interactions. The methyl groups of Met^{1}, Ala^{36}, Ala^{108}, and Leu^{117}, as well as the side chain of Pro^{37}, form a hydrophobic pocket for Tyr^{115} as evidenced by a large number of direct NOE observations between these residues. In addition to Tyr^{115} and Leu^{117}, most of the carboxyl-terminal residues are involved in numerous direct NOE-observable contacts to residues of the amino terminus and the loop connecting β-strands $\beta1$ and $\beta2$. Thus, clearly the carboxyl-terminal residues of GABARAP are an integral part of the globular and compact structure of GABARAP.

Throughout the GABARAP and GATE-16 family of proteins, Phe^{115} appears to be highly conserved (4). GABARAP itself and a *Caenorhabditis elegans* ortholog of GATE-16 are the only remarkable exceptions, containing a tyrosine at this position. Stabilizing the closed conformation of the carboxyl terminus in the GABARAP solution structure using a hydrogen bond in addition to hydrophobic interactions might therefore be a unique feature of GABARAP that is, however, not observed in the reported crystal structure. ^{1}H-^{15}N NOE data confirm that Tyr^{115} does not exhibit a decreased heteronuclear NOE (Fig. 2*B*) as would be expected for a residue not rigidly connected to the globular fold of the protein.

The carboxyl terminus of GABARAP may play a decisive role in the biological function of the protein. GABARAP as well as GATE-16, MAP-LC-3, and human Apg12p were shown to be substrates for human Apg7p, a novel E1 enzyme essential for the Apg12p-conjugating system (21), a system involved in autophagy. Autophagy is a process that involves the bulk degradation of cytoplasmic components by the lysosomal/vacuolar system, which is conserved from yeast to mammalian cells. For the yeast system, it was shown that Apg12p is covalently attached to Apg5p via the carboxyl-terminal glycine residue of Apg12p, which is very similar to the ubiquitin system (22). Apg12p is a homologue to GATE-16 and GABARAP. If indeed GABARAP plays a role in these kinds of covalent modification systems, its carboxyl terminus needs to be accessible during this process.

The two conformations found for GATE-16 were discussed already in regard to a potential role of the carboxyl terminus as a regulating element for modulating binding events (4). Transferred to GABARAP, this could mean that the solution structure of GABARAP resembles the conformation of free and unliganded GABARAP. The crystal structure of GABARAP may indicate the existence of a second conformation with its carboxyl terminus detached from the major part of the protein with an increased accessibility for the carboxyl-terminal residues.

Taking all observations together, it seems that the amino-terminal part of GABARAP exists in a state that allows at least two different conformations. Any decision between either one of them, *e.g.* upon tubulin binding, may influence subsequently the orientation of the closely attached carboxyl-terminal region of the protein. Its different orientations in the structures reported so far strongly suggest that this part of GABARAP is able to exist in various orientations relative to the rest of the protein. Such a direct conformational communication between a potentially interaction-sensitive region (residues *highlighted* in Fig. 1*C*) with a distant region of the protein is, however, a speculation that needs to be addressed by future investigations.

This kind of triggered conformational change may also be used for rational manipulation of GABARAP function. Selective stabilization of the conformation with a tightly attached carboxyl terminus may inhibit binding to interaction partners.

Acknowledgment—We thank C. Beck for technical assistance.

REFERENCES

1. Wang, H., Bedford, F. K., Brandon, N. J., Moss, S. J., and Olsen, R. W. (1999) *Nature* **397,** 69–72
2. Kneussel, M., Haverkamp, S., Fuhrmann, J. C., Wang, H., Wassle, H., Olsen, R. W., and Betz, H. (2000) *Proc. Natl. Acad. Sci. U. S. A.* **97,** 8594–8599
3. Okazaki, N., Yan, J., Yuasa, S., Ueno, T., Kominami, E., Masuho, Y., Koga, H., and Muramatsu, M. (2000) *Brain Res.* **85,** 1–12
4. Paz, Y., Elazar, Z., and Fass, D. (2000) *J. Biol. Chem.* **275,** 25445–25450
5. Kneussel, M., and Betz, H. (2000) *Trends Neurosci.* **23,** 429–435
6. Chen, L., Wang, H., Vicini, S., and Olsen, R. W. (2000) *Proc. Natl. Acad. Sci. U. S. A.* **97,** 11557–11562
7. Knight, D., Harris, R., McAllister, M. S. B., Phelan, J. P., Geddes, S., Moss, S. J., Driscoll, P. C., and Keep, N. H. (2002) *J. Biol. Chem.* **277,** 5556–5561
8. Coyle, J. E., Qamar, S., Rajeshankar, K. R., and Nikolov, D. B. (2002) *Neuron* **33,** 63–74
9. Stangler, T., Mayr, L. M., Dingley, A. J., Luge, C., and Willbold, D. (2001) *J. Biomol. NMR* **21,** 183–184
10. Zuiderweg, E. R., and Fesik, S. W. (1989) *Biochemistry* **28,** 2387–2391
11. Muhandiram, D. R., Farrow, N. A., Xu, G.-Y., Smallcombe, S. H., and Kay, L. E. (1993) *J. Magn. Res.* **102B,** 317–321
12. Farrow, N. A., Muhandiram, R., Singer, A. U., Pascal, S. M., Kay, C. M., Gish, G., Shoelson, S. E., Pawson, T., Forman-Kay, J. D., and Kay, L. E. (1994) *Biochemistry* **33,** 5984–6003
13. Johnson, B. A., and Blevins, R. A. (1994) *J. Biomol. NMR* **4,** 603–614
14. Nilges, M., and O'Donoghue, S. I. (1998) *Prog. NMR* **32,** 107–139
15. Nilges, M. (1993) *Proteins* **17,** 297–309
16. Brünger, A. T., Adams, P. D., Clore, G. M., DeLano, W. L., Gros, P., Grosse-Kunstleve, R. W., Jiang, J. S., Kuszewski, J., Nilges, M., Pannu, N. S., Read, R. J., Rice, L. M., Simonson, T., and Warren, G. L. (1998) *Acta Crystallogr. Sect. D Biol. Crystallogr.* **54,** 905–921
17. Koradi, R., Billeter, M., and Wüthrich, K. (1996) *J. Mol. Graph.* **14,** 51–55
18. Laskowski, R. A., MacArthur, M. W., Moss, D. S., and Thornton, J. M. (1993) *J. Appl. Crystallogr.* **26,** 283–291
19. Vriend, G. (1990) *J. Mol. Graph.* **8,** 52–56
20. Harris, R., McAllister, M. S. B., Sankar, A., Phelan, J. P., Moss, S. J., Keep, N. H., and Driscoll, P. C. (2001) *J. Biomol. NMR* **21,** 185–186
21. Tanida, I., Tanida-Miyake, E., Ueno, T., and Kominami, E. (2001) *J. Biol. Chem.* **276,** 1701–1706
22. Mizushima, N., Noda, T., Yoshimori, T., Tanaka, Y., Ishii, T., George, M. D., Klionsky, D. J., Ohsumi, M., and Ohsumi, Y. (1998) *Nature* **395,** 395–398